

IEA Wind Task 46

Erosion of wind turbine blades

Report on measurements of LEE drivers including metrology development and prospects for establishing 'super sites' for instrument testing the status of deployed measurement techniques

**Technical
report**



iea wind

Technical report 2.7: Report on measurements of LEE drivers including metrology development and prospects for establishing ‘super sites’ for instrument testing the status of deployed measurement techniques

**Prepared for the
International Energy Agency Wind Implementing Agreement**

**Prepared by
IEA Task 46 participants:**

Ebba Dellwik, DTU Wind and Energy Systems

Sara C Pryor, Cornell University

Charlotte Bay Hasager, DTU Wind and Energy Systems

Ásta Hannesdóttir, DTU Wind and Energy Systems

Rebecca J. Barthelmie, Cornell University

Joachim Reuder, University of Bergen

Marianne Rodgers, Wind Energy Institute of Canada

Robbie Sanderson, Wind Energy Institute of Canada

Heather Norton, Wind Energy Institute of Canada

February 2025

IEA Wind TCP functions within a framework created by the International Energy Agency (IEA). Views, findings, and publications of IEA Wind do not necessarily represent the views or policies of the IEA Secretariat or of all its individual member countries. IEA Wind is part of IEA's Technology Collaboration Programme (TCP).

Purpose

Leading edge erosion (LEE) of wind turbine blades has been identified as a major factor in decreased wind turbine blade lifetimes and energy output over time. Accordingly, the International Energy Agency Wind Technology Collaboration Programme (IEA Wind TCP) has created Task 46 to undertake cooperative research in the key topic of blade erosion. Participants in the task are given in Table 1.

The Task 46 under IEA Wind TCP is designed to improve understanding of the drivers of LEE, the geospatial and temporal variability in erosive events; the impact of LEE on the performance of wind plants and the cost/benefit of proposed mitigation strategies. Furthermore Task 46 seeks to increase the knowledge about erosion mechanics and the material properties at different scales, which drive the observable erosion resistance. Finally, the Task aims to identify the laboratory test setups which reproduce faithfully the failure modes observed in the field in the different protective solutions.

This report is a product of Work Package 2 **Climatic conditions driving blade erosion**.

The objectives of the work summarized in this report are to:

- To present considerations regarding how the different observational metrologies meet different needs in the field of precipitation erosion of wind turbine blade coatings.
- To summarize the experience by the working group regarding deployment of different precipitation sensors in view of the scientific literature.
- To look forward and formulate a future initiative for providing accurate information on the meteorological drivers for LEE.

Table 1. IEA Wind Task 46 Participants.

Country	Contracting Party	Active Organizations
Belgium	The Federal Public Service of Economy, SMEs, Self-Employed and Energy	Engie
Canada	Natural Resources Canada	WEICan
Denmark	Danish Energy Agency	DTU (OA), Hempel, Ørsted A/S, PowerCurve, Siemens Gamesa Renewable Energy
Finland	Business Finland	VTT
Germany	Federal Ministry for Economic Affairs and Energy	Fraunhofer IWES, Covestro, Emil Frei (Freilacke), Nordex Energy SE, RWE, DNV, Mankiewicz, Henkel
Ireland	Sustainable Energy Authority of Ireland	South East Technology University, University of Galway, University of Limerick
Japan	New Energy and Industrial Technology Development Organization	AIST, Asahi Rubber Inc., Osaka University, Tokyo Gas Co.
Netherlands	Netherlands Enterprise Agency	TU Delft, TNO
Norway	Norwegian Water Resources and Energy Directorate	Equinor, University of Bergen, Statkraft
Spain	CIEMAT	CENER, Aerox, CEU Cardenal Herrera University, Nordex Energy Spain
United Kingdom	Offshore Renewable Energy Catapult	ORE Catapult, University of Bristol, Lancaster University, Imperial College London, Ilosta, Vestas
United States	U. S. Department of Energy	Cornell University, Sandia National Laboratories, 3M

Table of Contents

Contents

1. Executive Summary	6
2. Why do we need observations on precipitation?	7
3. What types of sensors are there and how much data do they typically generate? 7	
4. How accurate are precipitation sensors?	9
5. Looking forward: establishments of ‘Super sites’	17
6. References.....	17

List of Figures

Figure 1. Boxplots of 4-years of 1-minute precipitation intensity as a function of the data integration (i.e. data averaging) period for a site in the US Southern Great Plains (see site description in Pryor et al. 2022). 8

Figure 2. Cumulative precipitation amounts for the year 2019 in Bergen, Norway derived from co-located disdrometer (Parsivel), MRR (METEK, post-processed by original METEK software and by RaProM), and a Geonor T-200B all-weather rain gauge. The Parsivel and RaProM data also distinguish between rain and snow, which is included in the graph (RR, RR + SR). 12

Figure 3. (a) Instruments deployed at the Wind Energy Institute of Canada (b) Scatterplot of hourly precipitation during summer months (May-October) from the tipping bucket rain gauge and disdrometer in 2022 and 2023. 13

Figure 4. Intercomparison of cumulative rain amount from two disdrometers and a RIMCO tipping-bucket rain gauge during a high-intensity rain event (left) and moderate-intensity (right). 13

Figure 5. DSD distributions from the two events in Figure 4. The two left and right panes correspond to data from the high and moderate rain-intensity events, respectively. Drops between the two dashed lines were used to recalculate the rain amount for the dashed curves in Figure 4. 16

Figure 6. The joint distributions of droplet diameter and fall velocity as reported by an OTT Parsivel², filtered for 3 different wind speed ranges and precipitation events where the 1-minute reported rainfall rate is 0.2–0.4 mm/h. For the highest wind speed case, we can see an occurrence of 1mm droplets with a negligible fall velocity. 17

List of Tables

Table 1. Key precipitation measurement techniques and their relative costs.	9
Table 2. Key precipitation measurement techniques and their main output parameter(s) and number of measured parameters. Derived parameters are indicated with parenthesis.	

1. Executive Summary

Leading edge erosion of wind turbine blade coatings is highly sensitive to hydroclimatic conditions and the joint probability distributions of wind and precipitation properties. Hence, co-located, repeatable and reliable precipitation and wind measurements at relevant turbine heights are needed to understand, quantify and – ultimately – mitigate or minimize leading edge erosion. While enormous strides have been made in measurement technologies in recent decades, instruments used to characterize hydroclimate conditions still exhibit relatively large uncertainty. This uncertainty, in turn, leads to highly significant variations in the life-time prediction of coatings used for leading edge protection. Therefore, there is a need to improve the available instruments, and identify which new options are the most suitable in the context of leading edge erosion applications. The working group suggests that such work can benefit from the establishments of ‘super-sites’. At such sites, comprehensive measurement campaigns including a range of metrologies for detection and quantification of hydroclimate parameters and wind conditions could be co-deployed.

2. Why do we need observations on precipitation?

In most environments, the erosion of wind turbine blade coatings is caused by material stresses, which - in turn - are primarily caused by impacts of hydrometeors, (liquid or solid water particles) on the rotating blades. To predict, understand and mitigate the erosion effects, there is need for observations of multiple aspects of the hydroclimate:

1. Precipitation climatologies for the planning phase when choosing the wind turbines and selecting whether (or not) to apply leading edge protection. These measurements should, at a minimum, include total annual accumulated precipitation and time-series of precipitation intensity and phase.
2. Hydrometeor-size distributions and phase (rain/hail) for the damage modeling of wind turbine blade coatings to evaluate the need for post-deployment LEP.
3. Severe weather and extreme precipitation warnings as decision-support for potential erosion-safe operation of wind turbines to reduce the rate of coating damage.

The damage potential of hydrometeors hitting a wind turbine blade is highly dependent on the relative speed of impact. Since the fall velocity of the hydrometeors are much smaller than the rotational speed of the turbine blade and the rotational speed depends on the wind speed, the wind energy sector needs to quantify the joint occurrence of wind speeds and precipitation events (see, e.g., Pryor et al., 2022). Since these wind conditions are needed at the heights swept by the rotor, routine synop observational sites used with masts rarely exceeding 10 m height (WMO, 2023, [ASOS](#)), are not ideally suited for LEE research.

3. What types of sensors are there and how much data do they typically generate?

Precipitation is highly heterogeneous in space and time. The variations with time is illustrated in Figure 1 which emphasizes the importance of sampling (or integration) period on precipitation intensity. In addition to variations in time and space hydrometeors may take the form of liquid droplets or solid spheres (hail) and/or flakes (snow). Mixed phase precipitation events where hydrometeors falling at a given location are both distributed in diameter space (i.e. size) are also common. For a comprehensive review of precipitation theory, spatiotemporal variability, measurement technologies and modeling strategies, the reader is directed to Morbidelli (2022).

When designing a measurement campaign or a meteorological surveillance setup regarding precipitation, there are several different measurement technologies to choose among. Key precipitation measurement technologies and an approximate estimate of their relative costs are listed in Table 1 and the precipitation parameters and number of parameters are listed in Table 2. Precipitation types are, e.g. liquid such as rain, fog, drizzle and solid such as hail, graupel and snow see, e.g., <https://cloudatlas.wmo.int/en/hydrometeors.html>).

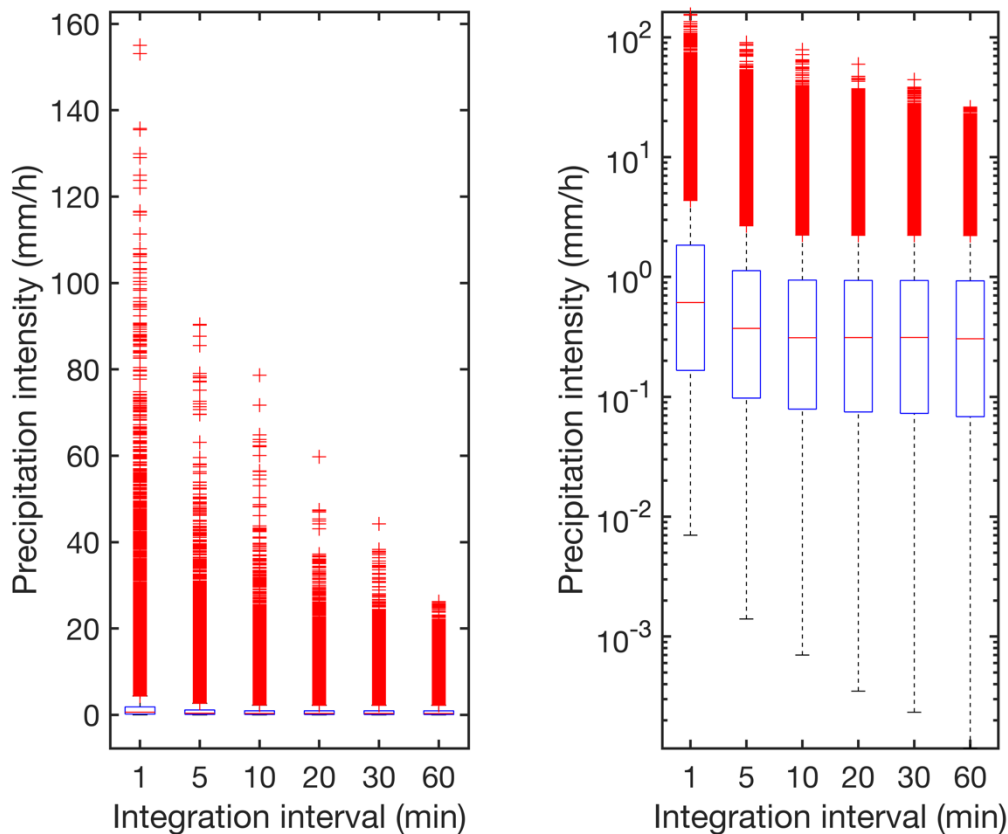


Figure 1. Boxplots of 4-years of 1-minute precipitation intensity as a function of the data integration (i.e. data averaging) period for a site in the US Southern Great Plains (see site description in Pryor et al. 2022). The precipitation intensity data are presented on a linear (left) and logarithmic axis (right) for different integration intervals. As shown, the maximum precipitation intensity in a 1-minute period is over 140 mm/hr while if these same data are averaged over 10-minute intervals the maximum intensity is < 80 mm/hr. The bottom and top of each box are the 25th and 75th percentiles of the sample, the horizontal line is the median, the whiskers extend to 1.5 times the inter-quartile range and observations beyond the whiskers are shown with plus symbols.

The depth of precipitation accumulated at the surface over a given time interval (the precipitation intensity) can be readily measured by a range of rain gauge technologies (Nystuen, 1996). Most national meteorological networks heat the collection funnel of the rain gauge to melt snow/solid precipitation and also employ wind shielding to prevent under-catch of snow/precipitation during high wind speeds (e.g., Kochendorfer et al. 2017). Multiple national weather services use dual polarization scanning Doppler RADAR for precipitation detection/ quantification and characterization (e.g. hydrometeor type). Similar technology but without dual polarization and scanning capabilities are employed in vertically-pointing micro-rain RADAR (Peters et al., 2005). While a systematic comparison of metrologies has not thus far been undertaken by this IEA Task 46 working group, considerable focus has been placed on disdrometer technologies (Pryor et al. 2022). These instruments discretize the hydrometeor population by diameter and work on one of three principles and yield measurements of:

- Optical (or laser) disdrometers detect the number concentration by both the diameter and fall velocities of hydrometeors.

- Impact disdrometers detect acoustic emissions from hydrometeors hitting a drum and by assuming each is falling at its terminal fall velocity infer the number concentration by diameter.
- 2-D video disdrometers track multiple dimensions of the hydrometeor population including diameter, fall velocity and asymmetry (axis ratio).

Table 1. Key precipitation measurement techniques and their relative costs.

Sensor type	Technological principle	Relative cost
Rain detection	Voltage over plate / optical.	\$
Rain gauge	Weight or tipping bucket	\$\$-\$
Disdrometer	Laser-based / optical / acoustic / video	\$\$-\$\$\$
Rain radars (vertically pointing and or dual-polarization scanning Doppler)	Reflection of microwaves	\$\$-\$\$\$\$

Table 2. Key precipitation measurement techniques and their main output parameter(s) and number of measured parameters. Derived parameters are indicated with a parenthesis.

Sensor type	Yes/No	Rain intensity (depth/time)	Droplet-diameters (length)	Droplet fall velocities (length/time)	Precipitation type	Number of measured parameters
Rain detection	X					1
Rain gauge		x				1
Disdrometer		x	x	x	x	>1000
MicroRain Radars (MRR)		(x*)	(x**)	x	(x***)	>100

4. How accurate are precipitation sensors?

4.1 Selected Results from the Meteorology and Hydrology literature

Systematic observations with several co-located and highly maintained precipitation sensors have primarily been undertaken by scientists working in the field of

meteorology or hydrology, where, naturally, precipitation accuracy is of immense importance. Below, we list a few of these studies and their key results.

Under the umbrella of the World Meteorological Organisation (WMO), Lanza and Stagi (2009) argue that measurement errors in rain gauges can relatively easily become as low as 1%. This conclusion was based on an extensive laboratory intercomparison. Later on, the same authors released their final intercomparison results from a field intercomparison (Lanza et al. 2010), highlighting the need for post-processing of rain gauges to reach the WMO accepted limit of 5% uncertainty in the rain amount measurements. The authors further concluded that the tested disdrometers did not reach this accuracy.

A few years later, the company OTT Hydromet released a new version of their disdrometer called Parsivel². An intercomparison with the first version of the instrument, a second disdrometer of a different manufacturer, as well as two rain gauges was presented by Tokay et al. (2014). They noted an improvement in the new version of the instrument, since the absolute bias in total rain amount measured over 36 rain events was reduced from 15% to 6% in comparison to the reference rain gauge. The authors also emphasized the importance of constructive communication between the instrument manufacturer and its users when diagnosing and correcting instrumental issues.

In 2018, Angola-Martinés et al. presented a disdrometer intercomparison, where they used two Parsivel² instruments and two disdrometers produced by the company Thies Clima. The study results showed significant differences between the OTT and Thies Clima sensors, and moreover that this difference grew with increasing rain intensity. The authors also highlighted the need for removing droplets that were likely caused by instrumental errors from the rain intensity calculation.

A year later, Jash et al. (2019) presented a comparison of drop-sizes and rain rates from a co-located micro-rain radar (MRR, Metek GmbH, Germany) and a disdrometer (OTT Parsivel-1, OTT Hydromet, Germany). This study was concluded with the sentence: *“The study reveals that in heavy rainfall conditions there is significant disparity in rain integral parameters between disdrometer and MRR measurements which arises due to the laser inhomogeneity problem of disdrometer, difference in measurement principles and the attenuation of MRR signal at different altitude levels.”* A step towards reducing the difference between the two instruments was demonstrated by (Garcia-Benadi et al., 2020), who used data from a field experiment in the eastern Pyrenees, where two automatic weather stations, a Parsivel² disdrometer and a MRR were deployed. Based on the collected data, new algorithms were developed for enabling a precipitation type classification in the MRR. The algorithm takes a reference rain intensity as input, and outputs a calibration of the original rain rate estimated from the MRR, in addition to the classification. The recommended algorithm can be found in an open-source software, as a Python language program called RaProM in a public github repository.

A major, and currently unresolved, issue with processing of data from optical disdrometers is the occurrence of droplets that are reported with fall velocities and horizontal diameters that differ from expectations. Specifically, the presence of large diameter but slowly falling hydrometeors. While snow exhibits these joint properties, such reports exist even during warm periods when snow cannot be present. This issue is discussed further below and is well-known within the atmospheric science

literature (see review in Letson and Pryor, 2023). However, best practice for how to treat such observations is missing.

In contrast to best-practice from rain-gauge networks, most disdrometers are not typically deployed using wind-shielding. However, lateral advection of hydrometers within the viewing area of some disdrometers during high wind speeds leads to biases in both the inferred fall velocity and diameters and thus the precipitation rate (e.g. Capozzi et al., 2021), although this effect was found to be relatively modest at near-surface wind speeds below 12 ms⁻¹ during a recent experiment using wind shielding of a disdrometer (Pryor et al. 2024).

In summary, all of studies cited above and many more within the scholarly literature highlight both the importance and the challenges of measuring precipitation characteristics of relevance to wind turbine blade coating erosion accurately.

4.2 Wind-energy context

In an overview paper covering the LEE aspects from the fields of meteorology, aerodynamics, materials science and computational mechanics, Mishanevsky et al. (2020) highlighted the need for high-frequency and high-resolution hydrometeor size distribution measurements from disdrometers. That study and many others (e.g., Dolan et al., 2018) have illustrated important differences in hydrometeor size distributions collected in different geographic/climate contexts (e.g., off-shore and on-shore), and emphasized the need for more off-shore observations, where the leading edge erosion is expected to be associated with largest repair costs.

In a study on how the kinetic energy of rain drops change over season Tilg et al (2021) used data from a site with six rain gauges and one disdrometer. The recorded rain drops by the disdrometer were filtered based on thirteen criteria. From this filtered dataset, the rain rate was re-calculated and compared to that of the rain gauges (an illustration of such data treatment can be seen in Figures 4 and 5, below). Despite the careful data filtering, the disdrometer showed the highest recorded rain amount among all the rain observations, indicating a positive bias.

Another aspect concerning accuracy was shown by Pryor et al. (2022), who analysed six observational datasets of disdrometer rain rates and drop-size distributions (DSD). The rain rates were classified according to wind speed classes, thereby emphasizing the wind energy specific angle. Concerning the observed DSDs, they were compared to existing literature, focussing on the DSD used in laboratory experiments of material fatigue. The study showed that the so-called Best DSD being recommended for use in whirling arm experiments did not represent the observational data, which emphasizes the need for improved DSD models.

In a follow-up instrumental intercomparison, Letson and Pryor (2023) demonstrated how the disagreement in DSDs and precipitation rates from three different disdrometers; optical (laser), impact and 2-D video disdrometers strongly affected the kinetic energy of the hydrometeor impacts on the blade. Estimates of total kinetic energy of hydrometeor impacts over the four-year data period varied by 38% and coating lifetime derived from the Springer model differ by >70% depending on disdrometer type. This finding underlines the need for observational accuracy.

In the working group meetings, we discussed the different setups and results from the instruments in a wind energy context. Because of the extensive data output from the disdrometers (Table 3), and the extensive need for data post-processing summarized, e.g., by Tilg et al (2021), these observations were often in focus of the discussions. A few results are shown here to underline, illustrate and extend the conclusions from the published studies.

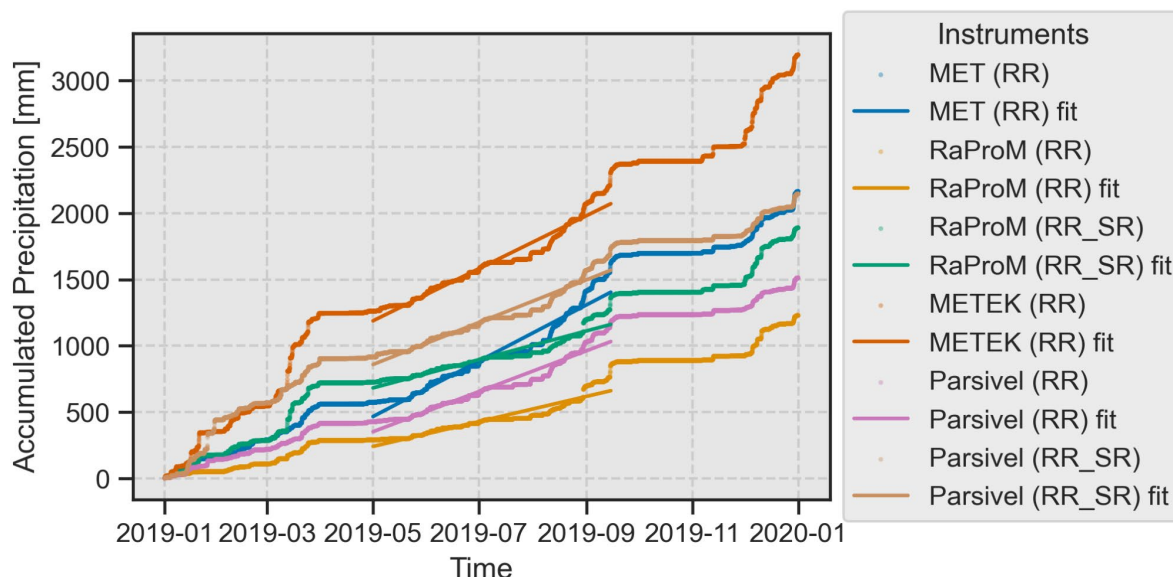


Figure 2. Cumulative precipitation amounts for the year 2019 in Bergen, Norway derived from co-located disdrometer (Parsivel), MRR (METEK, post-processed by original METEK software and by RaProM), and a Geonor T-200B all-weather rain gauge. The Parsivel and RaProM data also distinguish between rain and snow, which is included in the graph (RR, RR + SR).

The analysis of a long-term MRR data set collected in Bergen, Norway (Möller, 2024) indicates that the RaProM post-processing software (Garcia-Benadi et al., 2020), offering a distinction between rainfall rate (RR) and snow rate (SR), provides a reasonable classification of liquid hydrometeors when compared with the classification provided by the Parsivel disdrometer (Figure 2). However, RaProM struggles with the correct classification of solid hydrometeors (hail, snow) and drizzle, an issue also highlighted by Garcia-Benadi et al. (2020). In addition, a distinct underestimation of the total annual precipitation amount by RaProM in the order of 80 % was found, indicating a potential rain climate dependent tuning of the RaProM algorithm.

The Wind Energy Institute of Canada (WEICan) measures precipitation with both an OTT Parsivel² optical disdrometer and a Campbell Scientific TE525 Tipping Bucket Rain Gauge on their wind farm in Prince Edward Island, Canada. The hourly precipitation during summer months (May-October) during 2022 and 2023 are reported in Figure 3. Even when winter months are excluded to avoid differences in the measurement of ice and snow, there are time periods of disagreement over a wide range of precipitation rates. Both sensors report non-zero measurements that are not detected by the other sensor. The hourly accumulated precipitation from the disdrometer tends to be lower than for the tipping bucket. See also the work of Pryor et al. (2024).

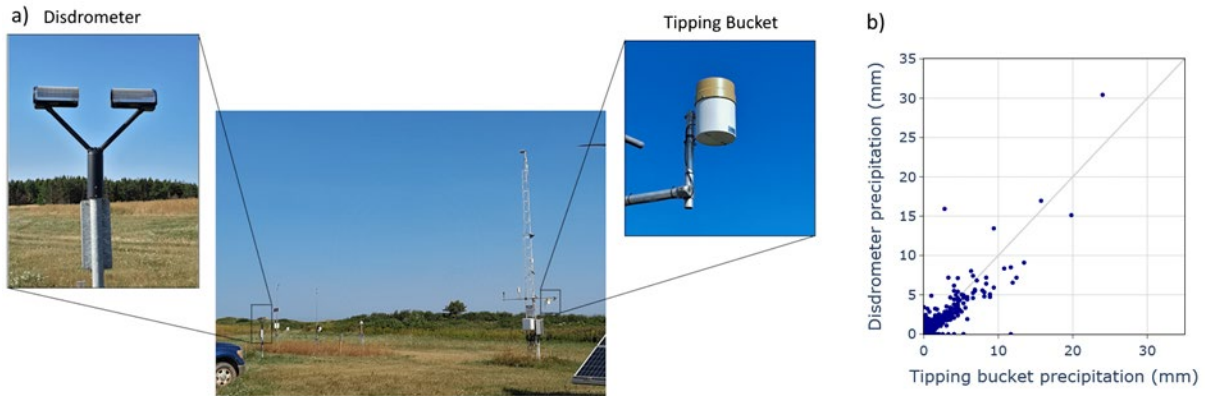


Figure 3. (a) Instruments deployed at the Wind Energy Institute of Canada (b) Scatterplot of hourly precipitation during summer months (May-October) from the tipping bucket rain gauge and disdrometer in 2022 and 2023.

The next example result is based on a setup at the Risø Campus in Roskilde, Denmark. Here, DTU operates two disdrometers, a Laser Precipitation Monitor (LPM) by Thies Clima and a Parsivel² by Ott Hydromet, and a tipping-bucket rain gauge (RIMCO). Instead of looking at an overall comparison, as was done in Figure 3, we here zoom in on two events: one with very high rain intensities (Figure 4, left) and one with moderate rain intensities (Figure 4, right). The three black and red lines in both plots denote different ways of estimating the rain amount from the Parsivel² and the LPM, respectively, whereas the full blue lines correspond to the results from a tipping-bucket rain gauge.

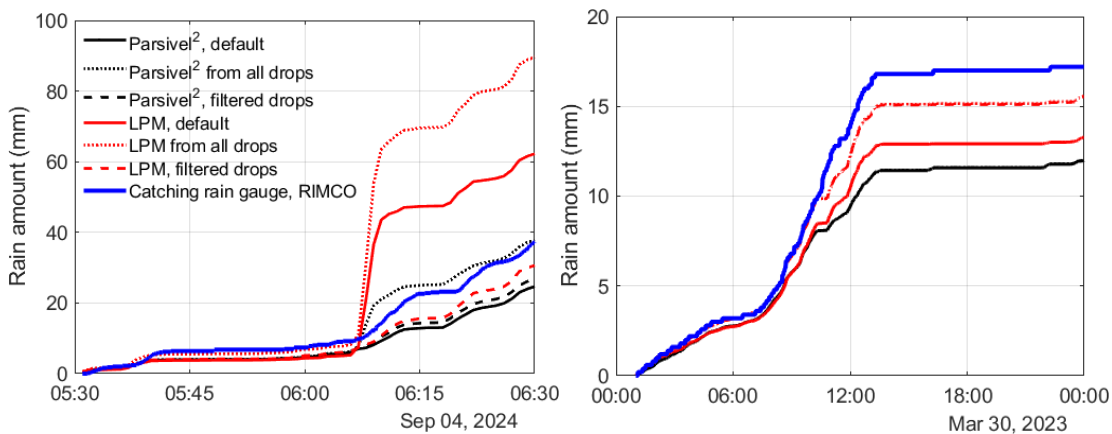


Figure 4. Intercomparison of cumulative rain amount from two disdrometers and a RIMCO tipping-bucket rain gauge during a high-intensity rain event (left) and moderate-intensity (right).

The results clearly show strong differences between the tested instruments, and, further, that the default rain rate output by the instruments (full lines) is often drastically different if either all or a filtered selection of the drops are used in the precipitation rate calculation (dashed and dotted lines, respectively). For the high-intensity event, it is evident that both instruments use some filter to remove droplets before estimating the rain rates because the dotted lines (precipitation rate corresponding to all droplets) lie above the full lines.

To analyze these two events further, the raw recordings of the DSDs for the two events are shown in Figure 5. In the top row, the results for the LPM are shown, whereas the bottom row corresponds to those from the Parsivel². A prominent difference between the instruments is that the LPM records many more small droplets than the Parsivel² both for the high-intensity (left) and the moderate-intensity (right) events, and, further, these droplets fall with a high velocity. The occurrence of such small-diameter high-velocity combinations is a well-known problematic feature of the LPM (e.g., Angulo-Martínez et al., 2018) and is generally considered to be an instrumental error. To avoid that these droplets count in rain amount calculations, filters are introduced, as mentioned above. These filters are often based on a maximum deviation from other datasets, which are considered to correctly reflect the fall velocity of rain drops of different diameters. The most commonly used standard is an 86 year old laboratory observation by Gunn and Kinzer (1949). Their expression is, for example, used by Letson and Pryor (2023) and an approximation to the same data by Atlas et al. (1973), is shown in Figure 5 as the full black line. Another standard is based on theoretical considerations regarding the drag coefficients of idealized drops (Beard, 1976) with the assumption that droplets fall at the terminal fall velocity in stagnant air. This approach was, for example, used by Angulo-Martínez et al (2018) to filter out droplets of unlikely diameter-fall velocity combinations. The Beard model has an advantage that variations in air density can be taken into account, which could be useful for MRR observations taken far from the surface. Both standards are based on how droplets behave in idealized conditions, which may not reflect the likely chaotic non-equilibrium conditions of real rain events.

These results underline the conclusion by Letson and Pryor (2023) regarding the lack of a transparent standard for how drops should be filtered. Because the sum of the volumes of the recorded drops does not correspond to the rain rate parameter from the instrument, it is, further, not clear how to use the raw data for improvement of DSD models.

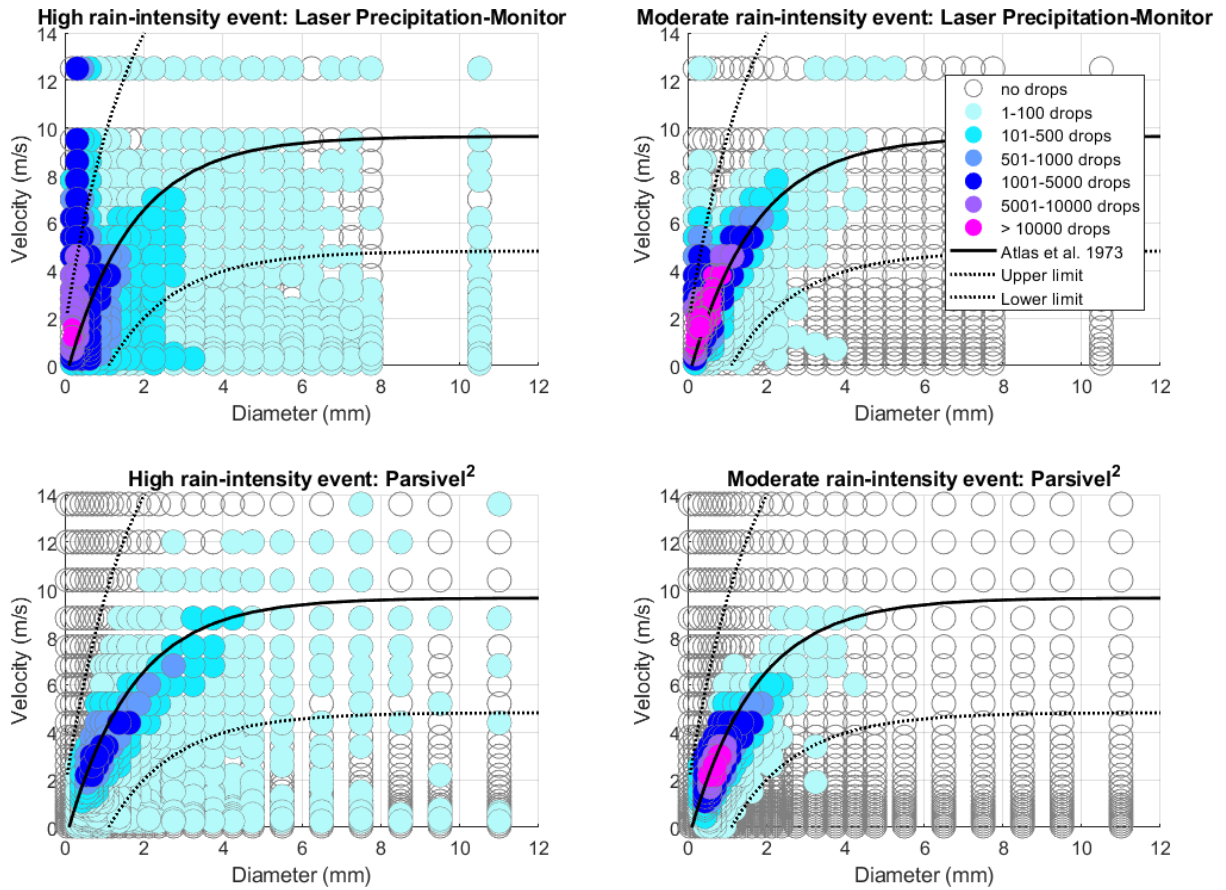


Figure 5. DSD distributions from the two events in Figure 4. The two left and right panes correspond to data from the high and moderate rain-intensity events, respectively. Drops between the two dashed lines were used to recalculate the rain amount for the dashed curves in Figure 4.

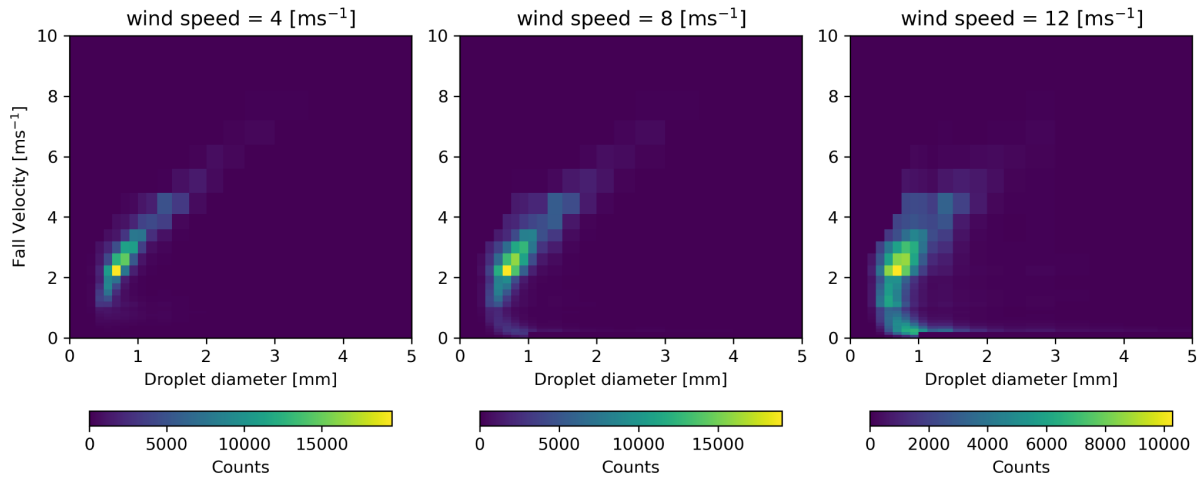


Figure 6. The joint distributions of droplet diameter and fall velocity as reported by an OTT Parsivel², filtered for 3 different wind speed ranges and precipitation events where the 1-minute reported rainfall rate is 0.2–0.4 mm/h. For the highest wind speed case, we can see an occurrence of 1mm droplets with a negligible fall velocity.

A last example from the working group is given in Figure 6 that shows the joint distribution of droplet diameter and fall velocity from a Parsivel² disdrometer mounted on top of a 122 m tall meteorological mast, also at the DTU Risø campus. These measurements were filtered for three different wind speed ranges: 4 ± 1 m/s, 8 ± 1 m/s, and 12 ± 1 m/s. To ensure consistency, the data are also filtered for rainfall intensity between 0.2–0.4 mm/h, as measured by the catching rain gauge at ground level. Wind directions parallel to the disdrometer were excluded due to shadowing effects from the disdrometer heads, which can prevent small droplets from reaching the laser plane (Capozzi et al. 2021). These three filters resulted in 172, 417 and 237 10-minute samples for the three wind speed intervals. The results indicate that higher wind speeds tend to be associated with more ‘unphysical’ or erroneous values where large droplet diameters correspond to near-zero fall velocities. These values are typically filtered out by applying range limits based on the theoretical relationship between fall velocity and droplet diameter.

A final reference is given to Caboni et al (2024), who stated regarding their use of standard disdrometers: “During our measurement campaign, we faced numerous challenges tied to the use of disdrometers, especially in offshore conditions. These include: corrosion issues, uncertainty in sensor calibration and possible measurement errors (e.g., interactions with insects, water particles rising from the sea and flow field effects around the sensors). Indeed, we attempted to collect rain measurements at two additional offshore locations, but unfortunately the disdrometers suffered from corrosion which invalidated the measurements”. This statement reflects that the need for detailed precipitation characterization emphasized by Mishanovsky et al. (2020) cannot easily be met.

In summary, the existing literature and work within the IEA Task 46 working indicate that in terms of accuracy, user-friendliness and robustness, existing precipitation instrumentation does not meet the needs of the wind energy LEE community.

5. Looking forward: establishments of ‘Super sites’

More research is needed to identify and evaluate robust instruments for wind energy related leading edge erosion research, and it is the recommendation of the working group members that well-instrumented ‘super sites’ at wind energy relevant locations be established for this purpose. This type of experimental design has been employed within other IEA Tasks (e.g. for lidar intercomparison e.g. https://iea-wind.org/wp-content/uploads/2023/10/59_Remote-Sensing-2_v2.p). At such sites, comprehensive measurement campaigns including a range of metrologies for detection and quantification of hydroclimate parameters and wind conditions could be co-deployed.

The goals of these coordinated experiments are as follows:

- Evaluate the performance of different types of instrumentation and quantify instrument closure through time and as a function of precipitation type/event intensity. Given the hail is an important damage vector for wind turbine blades (and other things including solar panels), it would be useful to include hail sensors within the instrument suite.
- To advance best practice for instrument deployment and data analyses protocols.
- Evaluate instrument reliability and ease of deployment and maintenance.
- Evaluate and identify instruments that are robust enough to cope with the harsh meteorological conditions, especially of off-shore sites.

To minimize errors in erosion predictions, the super sites should include wind observations should be taken at the heights swept by the rotor, i.e., at levels that are an order of magnitude higher than typical meteorological networks operated by meteorological institutes. For simple terrain sites, these conditions may be possible to relax, since recent comparisons between lidar wind profiler observations and reanalysis/hindcast data sets indicate that the latter have a significant potential to provide the required wind speed estimates when direct measurements are not available (Cheynet et al., 2024).

Whereas land sites are preferable for logistical reasons (e.g. ease of access), the marine boundary layer is also highly relevant for offshore wind farms and there is value in improved quantification of precipitation conditions over the ocean. Use of coastal sites may help to balance these considerations.

6. References

Angulo-Martínez, M., Beguería, S., Latorre, B., & Fernández-Raga, M. (2018): Comparison of precipitation measurements by OTT Parsivel 2 and Thies LPM optical disdrometers. *Hydrology and Earth System Sciences*, **22**(5), 2811-2837.

<https://doi.org/10.5194/hess-22-2811-2018>

Atlas, D., R. C. Srivastava, and R. S. Sekhon (1973): Doppler radar characteristics of precipitation at vertical incidence, *Rev. Geophys.*, 11(1), 1–35, <https://doi.org/10.1029/RG011i001p00001>

Beard, K. V. (1976): Terminal Velocity and Shape of Cloud and Precipitation Drops Aloft. *J. Atmos. Sci.*, **33**, 851–864, [https://doi.org/10.1175/1520-0469\(1976\)033<0851:TVASOC>2.0.CO;2](https://doi.org/10.1175/1520-0469(1976)033<0851:TVASOC>2.0.CO;2).

Caboni, M., Slot, H.M, Bergmann, G, Wouters, D.A.J. and Van Der Mijle Meijer, H.J. (2024): Evaluation of wind turbine blades' rain-induced leading edge erosion using rainfall measurements at offshore, coastal and onshore locations in the Netherlands *J. Phys.: Conf. Ser.* **2767** 062003, <https://doi.org/10.1088/1742-6596/2767/6/062003>

Capozzi, V., Annella, C., Montopoli, M., Adirosi, E., Fusco, G., & Budillon, G. (2021): Influence of Wind-Induced Effects on Laser Disdrometer Measurements: Analysis and Compensation Strategies. *Remote Sensing*, *13*(15), 3028. <https://doi.org/10.3390/rs13153028>

Cheyne, E., Diezel, J. M., Haakenstad, H., Breivik, Ø., Peña, A., and Reuder, J.(2025): Tall Wind Profile Validation Using Lidar Observations and Hindcast Data, *Wind Energ. Sci. Discuss.* [preprint], <https://doi.org/10.5194/wes-2024-119>, accepted for publication

Dolan, B., Fuchs, B., Rutledge, S. A., Barnes, E. A., & Thompson, E. J. (2018): Primary modes of global drop size distributions. *Journal of the Atmospheric Sciences*, *75*(5), 1453-1476, <https://doi.org/10.1175/JAS-D-17-0242.1>

Garcia-Benadi, A., Bech, J., Gonzalez, S., Udina, M., Codina, B., & Georgis, J.-F. (2020): Precipitation Type Classification of Micro Rain Radar Data Using an Improved Doppler Spectral Processing Methodology. *Remote Sensing*, *12*(24), 4113. <https://doi.org/10.3390/rs12244113>

Gunn, R.; Kinzer, G.D. (1949): The terminal velocity of fall for water droplets in stagnant air. *J. Atmos. Sci.*, **6**, 243–248, [https://doi.org/10.1175/1520-0469\(1949\)006<0243:TTVOFF>2.0.CO;2](https://doi.org/10.1175/1520-0469(1949)006<0243:TTVOFF>2.0.CO;2)

Jash, D., Resmi, E.A., Unnikrishnan, C.K., Sumesh, R.K., Sreekanth, T.S., Sukumar, N., Ramachandran, K.K. (2019): Variation in rain drop size distribution and rain integral parameters during southwest monsoon over a tropical station: An inter-comparison of disdrometer and Micro Rain Radar, *Atmospheric Research*, *217*, 24-36, <https://doi.org/10.1016/j.atmosres.2018.10.014>

Kochendorfer, J., Rasmussen, R., Wolff, M., Baker, B., Hall, M. E., Meyers, T., Landolt, S., Jachcik, A., Isaksen, K., Brækkan, R., and Leeper, R. (2017): The quantification and correction of wind-induced precipitation measurement errors, *Hydrol. Earth Syst. Sci.*, **21**, 1973–1989, <https://doi.org/10.5194/hess-21-1973-2017> .

Lanza, L. G., Stagi, L.(2009): High resolution performance of catching type rain gauges from the laboratory phase of the WMO Field Intercomparison of Rain Intensity Gauges, *Atmospheric Research*, **94**(4), 555-563, <https://doi.org/10.1016/j.atmosres.2009.04.012>

Lanza, L. G., Vuerich, E., and Gnecco, I.(2010): Analysis of highly accurate rain intensity measurements from a field test site, *Adv. Geosci.*, 25, 37–44, <https://doi.org/10.5194/adgeo-25-37-2010>

Letson, F.; Pryor, S.C. From Hydrometeor Size Distribution Measurements to Projections of Wind Turbine Blade Leading-Edge Erosion. *Energies* 2023, 16, 3906. <https://doi.org/10.3390/en16093906>

Mishnaevsky L, Hasager CB, Bak C, Tilg A-M, Bech JI, Doagou Rad S and Fæster, S. (2021): Leading edge erosion of wind turbine blades: Understanding, prevention and protection. *Renew Energy*; **169**:953–69, <https://doi.org/10.1016/j.renene.2021.01.044>

Morbidelli, R. (2022). *Rainfall : modeling, measurement and applications*. Elsevier. <https://www.sciencedirect.com/science/book/9780128225448>

Möller, F. (2024). *Hydrometeors and Their Impact on Leading Edge Erosion of Wind Turbine Blades - Evaluating the Effectiveness of the RaProM Software in Classifying Hydrometeor Types, or: How Complex Must Impingement Calculations Be for Accurate Erosion Estimations?* Master's thesis, University of Bielefeld. 173pp

Nystuen, J. A. (1999): Relative Performance of Automatic Rain Gauges under Different Rainfall Conditions. *J. Atmos. Oceanic Technol.*, **16**, 1025–1043, [https://doi.org/10.1175/1520-0426\(1999\)016<1025:RPOARG>2.0.CO;2](https://doi.org/10.1175/1520-0426(1999)016<1025:RPOARG>2.0.CO;2).

Peters, G., B. Fischer, H. Münster, M. Clemens, and A. Wagner (2005): Profiles of Raindrop Size Distributions as Retrieved by Microrain Radars. *J. Appl. Meteor. Climatol.*, **44**, 1930–1949, <https://doi.org/10.1175/JAM2316.1>

Pryor, S. C., Barthelmie, R. J., Cadence, J., Dellwik, E., Hasager, C. B., Kral, S. T., Reuder, J., Rodgers, M., & Veraart, M. (2022). Atmospheric Drivers of Wind Turbine Blade Leading Edge Erosion: Review and Recommendations for Future Research. *Energies*, **15**(22), Article 8553. <https://doi.org/10.3390/en15228553>

Pryor S.C., Barthelmie R.B., Coburn J.J., Zhou X., Rodgers M., Norton M., Campobasso M.S., Lopez B.M., Hasager C.B., and Mishnaevsky Jr L. (2024):

Prioritizing Research for Enhancing the Technology Readiness Level of Wind Turbine Blade Leading Edge Erosion Solutions. *Energies*, **17** 6285, <https://doi.org/10.3390/en17246285>

Tilg, A., F. Vejen, C. B. Hasager, and M. Nielsen (2020): Rainfall Kinetic Energy in Denmark: Relationship with Drop Size, Wind Speed, and Rain Rate. *J. Hydrometeor.*, 21, 1621–1637, <https://doi.org/10.1175/JHM-D-19-0251.1>

Tokay, A., D. B. Wolff, and W. A. Petersen (2014): Evaluation of the New Version of the Laser-Optical Disdrometer, OTT Parsivel2. *J. Atmos. Oceanic Technol.*, **31**, 1276–1288, <https://doi.org/10.1175/JTECH-D-13-00174.1>

WMO, Guide to Instruments and Methods of Observation (2023): WMO-No. 8, <https://library.wmo.int/viewer/68695/?offset=3#page=228&viewer=picture&o=bookmark&n=0&q=>